

## Shift in ENSO Teleconnections Recorded by a Northern Red Sea Coral

N. RIMBU, G. LOHMANN, T. FELIS, AND J. PÄTZOLD

*Department of Geosciences, Bremen University, Bremen, Germany*

(Manuscript received 25 March 2002, in final form 2 October 2002)

### ABSTRACT

El Niño–Southern Oscillation (ENSO) teleconnections over Europe and the Middle East are evaluated using an oxygen isotope coral time series from the northern Red Sea and various instrumental datasets. A shift in the correlation between the Niño-3 index and the Red Sea coral record in the 1970s is detected, and it is shown that this shift can be attributed to nonstationary circulation regimes and related ENSO teleconnections. It is found that positive anomalies of oxygen isotope in the Red Sea coral record from the middle 1930s to the late 1960s are associated with a strong Pacific–North Atlantic teleconnection accompanied by a weak Aleutian low, a more zonal flow at midlatitudes, and La Niña conditions in tropical Pacific. In contrast, positive anomalies of oxygen isotopes in the Red Sea coral after the 1970s are related to El Niño conditions and weaker Pan-Pacific–Atlantic circulation regimes. Using the window correlation of the northern Red Sea coral record with two coral records from the tropical and subtropical Pacific, nonstationary relationships between the tropical Pacific and the European–Middle Eastern climate during the preinstrumental period are found. The results imply that the modulation of teleconnections at interdecadal timescales provides a limitation in the prediction and reconstruction of remote climate phenomena such as the ENSO impact over Europe.

### 1. Introduction

Massive corals from the Tropics and subtropics provide an archive of climate variations during the last few hundred years (Cole et al. 1993; Charles et al. 1997; Urban et al. 2000; Felis et al. 2000). Many coral-based climate reconstructions concentrate on the El Niño–Southern Oscillation (ENSO) phenomenon (Cole et al. 1993; Urban et al. 2000), the major source of interannual variability in the global climate system originating in the tropical Pacific (Huang et al. 1998). Although the ENSO impact throughout the Tropics is relatively well understood, the knowledge of its extratropical response is based on teleconnection patterns that are statistical in origin and derived from the relatively short period of instrumental observations. Recent studies (Urban et al. 2000; Evans et al. 2001; Rimbu et al. 2001) have shown that the variability in coral records is related to large-scale climatic phenomena suggesting a possible use of these corals to study atmospheric teleconnections in the preinstrumental period.

Conditions in the tropical Pacific Ocean can have significant connections with the midlatitude atmospheric circulation, particularly in winter (Hamilton 1988). Notable is a tendency for an intensification of the climatological standing wave pattern over the North Pacific

and North America during the warm tropical conditions associated with ENSO events. Part of this response is due to the Pacific–North American (PNA) pattern in the troposphere, which is enhanced by El Niños via the intensification of the Aleutian Low.

Observational studies (Fraedrich and Müller 1992; Fraedrich 1994; Pozo-Vázquez et al. 2001) report an ENSO impact on the European realm. A composite analysis based on El Niño events from the observational period (1888–1987) reveals a negative anomaly in sea level pressure (SLP) over central Europe with a zonal belt stretching from Ireland to the Black Sea and positive SLP anomalies over northern and northeastern Europe during the winter season (December to February). The sign of the SLP anomalies reverses for La Niña events (Fraedrich 1994). Consistent with these results, the regimes of cyclonic weather are more frequent in western and central Europe during the winters of El Niño events while the regimes of anticyclonic weather prevail over these regions during La Niña events. It is noted also that the European climate is influenced more strongly by La Niña than by El Niño events (Pozo-Vázquez et al. 2001).

Here, we analyze whether the relationship between tropical Pacific sea surface temperature (SST) anomalies and European climate can be regarded as stationary, that is, not changing significantly with time. There are some indications that the connection between the tropical Pacific and the European and Middle Eastern climate was not uniform since the beginning of the instrumental ob-

---

*Corresponding author address:* Dr. G. Lohmann, Department of Geosciences, Bremen University, P.O. 330 440, Bremen 28334, Germany.  
E-mail: gerrit@palmod.uni-bremen.de

servations in the nineteenth century. Correlating the winter SLP from Darwin, Australia, with SLP from several European meteorological stations during an 80-yr period, van Loon and Madden (1981) have found nonstationary teleconnections. Only the patterns from the second half of the twentieth century clearly show the structure of correlation as expected from Fraedrich's (1994) composites. Other studies concentrate on the ENSO impact on rainfall. Rodo et al. (1997) point out that the association between ENSO and rainfall on the Iberian Peninsula has significantly intensified in the second half of the twentieth century. Positive significant correlations between winter rainfall in Israel and the Niño-3 ( $5^{\circ}\text{N}$ – $5^{\circ}\text{S}$ ,  $90^{\circ}$ – $150^{\circ}\text{W}$ ) index are identified after the mid-1970s whereas during the 1930s to 1970s period the correlation is not significant (Price et al. 1998). Similar nonstationary behavior characterizes the relation between western Mediterranean rainfall and the Niño-3.4 ( $5^{\circ}\text{N}$ – $5^{\circ}\text{S}$ ,  $120^{\circ}$ – $170^{\circ}\text{W}$ ) index (Mariotti et al. 2002).

In order to study the extratropical ENSO response in the preinstrumental era, we analyze the circulation regimes related to interannual variability in a coral record from the northern Red Sea (Felis et al. 2000) in combination with two coral records from the Pacific (Linsley et al. 2000; Urban et al. 2000). These proxies will bring the question of the ENSO impact over Europe and related circulation regimes into a long-term context.

The paper is organized as follows. Datasets used in this study are shortly described in section 2. The relationship between interannual variability in the Red Sea coral record and tropical Pacific SST anomalies is discussed in section 3. The analysis is focused on a change in this relationship that occurred in the 1970s. Based on large-scale SST and atmospheric circulation patterns related to variability in the coral time series before and after the 1970s, a physical explanation of this shift is presented (section 3). Furthermore, the shift in ENSO teleconnections over Europe and the Middle East in the 1970s is evaluated in the instrumental records. Comparison with corals from the Pacific Ocean brings the ENSO teleconnections over Europe and the Middle East into a long-term context. Finally, the results are discussed and conclusions are drawn (section 4).

## 2. Data

A bimonthly resolution oxygen isotope record covering the period 1750–1995 was generated from a coral growing at Ras Umm Sidd, Egypt, ( $28.9^{\circ}\text{N}$ ,  $34.3^{\circ}\text{E}$ ) in the northern Red Sea (Felis et al. 2000), one of the few Northern Hemisphere subtropical regions of coral growth. The core was collected from a massive coral colony directly exposed to open-sea conditions. This provides a good representation of large-scale oceanic and atmospheric conditions at a coastal site. Oxygen isotope analysis of this coral core was performed at the stable isotope laboratory of the Department of Geosciences at Bremen University, Germany (Felis et al. 2000).

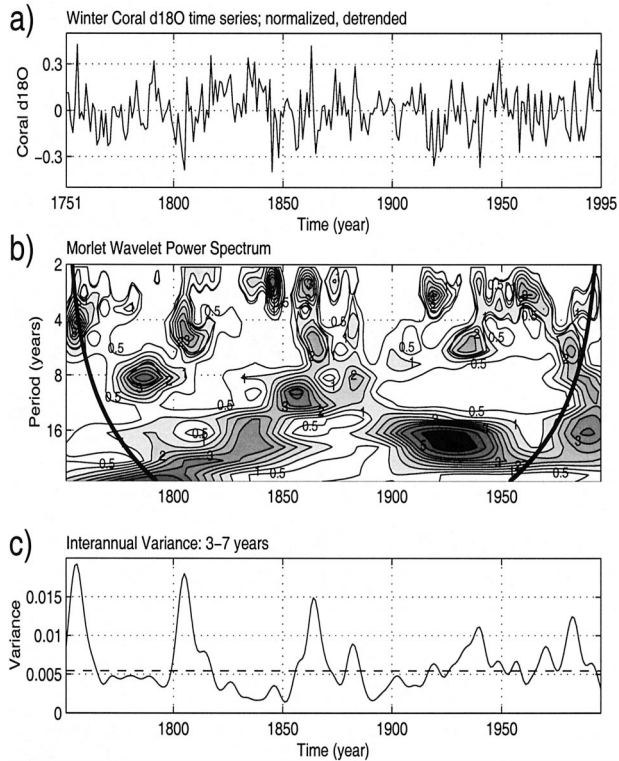


FIG. 1. (a) Winter (JF) time series (normalized, detrended) of the Ras Umm Sidd coral  $\delta^{18}\text{O}$  record (Felis et al. 2000) used for the wavelet analysis. (b) Morlet wavelet power spectrum. The shaded contours are at normalized variances of 0.5, 1.0, 1.5, 2.0, 2.5, 3.0, 3.5, 4.0, 5.0, 6.0, and 7.0. The thick line indicates the regions where edge effects become important. (c) Interannual variance (3–7 yr) of the coral  $\delta^{18}\text{O}$  time series.

The January–February (JF) values of each year are taken from this record in order to generate the wintertime series, shown in Fig. 1a. Although the ENSO signal over these regions is detectable in climatic data in all seasons of the year (Mariotti et al. 2002), we have concentrated our analysis on the winter (JF) season, when both interannual and decadal variability of the Red Sea coral record are related to large-scale atmospheric and oceanic processes (Rimbu et al. 2003). The ratio of the isotopic species of oxygen ( $^{18}\text{O}/^{16}\text{O}$ ) incorporated into coral skeletons during growth, reported as  $\delta^{18}\text{O}$ , is influenced by both the temperature and the  $\delta^{18}\text{O}$  of the ambient seawater during skeleton precipitation (Eshel et al. 2000; Felis et al. 2000). Variations in coral  $\delta^{18}\text{O}$  are therefore related to climate conditions and ocean circulation.

In order to evaluate the ENSO teleconnections over Europe and the Middle East in the preinstrumental era we use two coral records from the Pacific Ocean. The bimonthly resolution coral  $\delta^{18}\text{O}$  record from Maiana, in the tropical Pacific ( $1^{\circ}\text{N}$ ,  $173^{\circ}\text{E}$ ), covers the period 1840–1993 and is highly correlated with various ENSO indices (Urban et al. 2000). The other coral record is from Rarotonga, located in the subtropical South Pacific

(21°S, 160°W). The monthly resolution time series of coral strontium/calcium ratio (Sr/Ca) covers the period 1727–1996 and is a good proxy for local SST (Linsley et al. 2000). The decadal part of this time series has been used to understand Pacific decadal variability (Linsley et al. 2000; Evans et al. 2001). Here, we concentrate on the interannual variability of this coral record.

Prior to statistical analysis, we select the winter values of the coral time series for the considered period, remove the linear trend, calculate the anomalies against the mean over that period, and then normalize the series by their standard deviation.

For our analyses, we use several instrumental datasets. SST ( $1^\circ \times 1^\circ$ ) and surface wind ( $2.5^\circ \times 2.5^\circ$ ) for the period 1950–95 are taken from the Global Sea-Ice and SST data, version 2.3, (GISST2.3; Rayner et al. 1996) and National Centers for Environmental Prediction–National Center for Atmospheric Research (NCEP–NCAR) reanalysis (Kalnay et al. 1996) datasets. For the period 1856–1995, global SST ( $5^\circ \times 5^\circ$ ) are taken from the Kaplan dataset (Kaplan et al. 1998). Furthermore, we use SLP data over the Northern Hemisphere ( $5^\circ \times 5^\circ$ ) for the period 1899–1995 (Trenberth and Paolino 1980).

### 3. Results

#### a. Variability of the Red Sea coral record and its relation to ENSO

Because we want to address the question of nonstationarity of climate seen in the proxy time series, we perform a wavelet analysis (Torrence and Compo 1998) of the winter Red Sea coral  $\delta^{18}\text{O}$  record (Fig. 1a). By decomposing the time series into time–frequency space, we are able to determine both the dominant modes of variability and the evolution of these modes in time. The wavelet spectrum (Fig. 1b) of the linear detrended and normalized coral  $\delta^{18}\text{O}$  time series shows a strong nonstationary behavior. Several statistically significant (90% confidence level) bands of enhanced variability are detected: the interannual band (3–7 years), the decadal band (8–15 years), and the beyond-16-year band. When considering all timescales, we have found a correlation of 0.7 between this coral time series and the Arctic Oscillation index (Rimbu et al. 2001). Examining the variance in the interannual band (Fig. 1c), we find an amplitude modulation on a timescale of about 50–80 years in the Red Sea coral  $\delta^{18}\text{O}$  record.

In order to analyze the connection between the coral  $\delta^{18}\text{O}$  record and the ENSO phenomenon, we calculate the correlation coefficients between the coral time series and the Niño-3 index for a 20-yr moving window during the period 1856–1995. The Niño-3 index, which is used as a measure of the amplitude and phase of ENSO, is defined as the monthly SST averaged over the eastern half of the tropical Pacific ( $5^\circ\text{S}$ – $5^\circ\text{N}$ ,  $90^\circ$ – $150^\circ\text{W}$ ). The index used here is the version prepared by Kaplan et

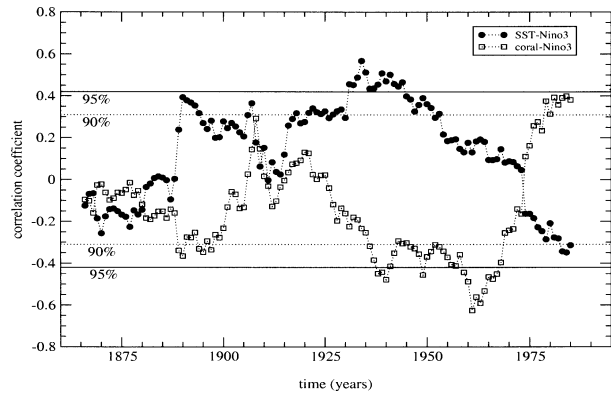


FIG. 2. The 20-yr running correlation coefficients between the winter (JF) time series of the Ras Umm Sidd coral  $\delta^{18}\text{O}$  record (Felis et al. 2000) and the Niño-3 index (open symbols) and between northern Red Sea SST and the Niño-3 index (solid symbols) for the period 1856–1995. Running correlation coefficients are plotted at the midpoint of each window; for example, the value at 1900 stands for the correlation during the period 1890–1910. The data were detrended and filtered in the 3–7-yr frequency interval prior to the correlation.

al. (1998). We updated this index from 1991 to 1995 by using data from the GISST2.3 dataset (Rayner et al. 1996). Prior to the correlation analysis both time series are linearly detrended, normalized, and filtered in the 3–7-yr frequency band (interannual timescales).

The resulting Fig. 2 shows a nonstationary behavior in the correlation between the Red Sea coral  $\delta^{18}\text{O}$  and the Niño-3 index time series on interannual timescales. Relatively high positive correlations are indicated for the windows centered after the mid-1970s, whereas relatively high negative correlations characterize the windows centered after the mid-1880s to the late 1890s, and after the mid-1930s to the late 1960s. Although the significance of the correlations for these windows is modest, the results are supported by a comparable behavior but of opposite sign in the correlation between northern Red Sea SST and the Niño-3 index, and therefore appear to be robust (Fig. 2). The opposite sign of the correlations is due to the inverse relation of coral  $\delta^{18}\text{O}$  and local SST (Eshel et al. 2000; Felis et al. 2000).

In the following we will concentrate on the physical processes that explain the shift from negative to positive correlations between the Niño-3 index and the Red Sea coral  $\delta^{18}\text{O}$  record that occurs in the 1970s (Fig. 2) and we will refer to it as the 1970s's shift. For the 20-yr windows centered after the mid-1930s to the late 1960s, that is, before the 1970s shift, positive anomalies in coral  $\delta^{18}\text{O}$  are associated with negative SST anomalies in the Niño-3 region. In contrast, after the 1970s shift, positive anomalies in coral  $\delta^{18}\text{O}$  are related to positive SST anomalies in the Niño-3 region.

#### b. Composite analysis of the coral record

In order to study the SST and atmospheric circulation patterns associated with interannual variability in the

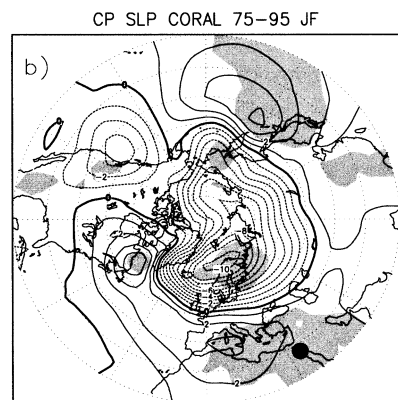
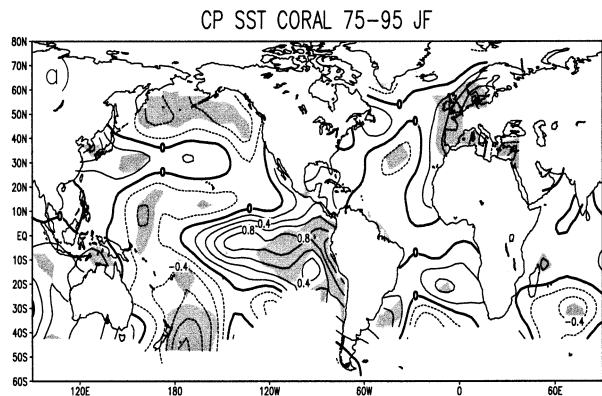


FIG. 3. Composite maps (difference between averaged maps for which JF Red Sea coral  $\delta^{18}\text{O}$  was higher/lower than 0.75 std dev) for (a) sea surface temperature (Kaplan et al. 1998) and (b) sea level pressure (Trenberth and Paolino 1980) for the period 1975–95. Shading indicates local statistical significance of the anomalies at 95% confidence level. The data were detrended and filtered in the 3–7-yr band prior to composite analysis. Units are K and hPa, respectively; the coral location is indicated by a black circle.

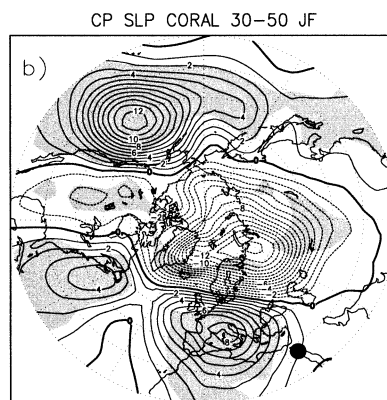
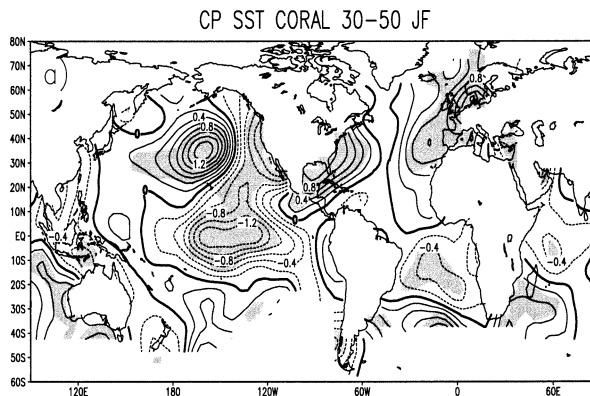


FIG. 4. As in Fig. 3, but for the period 1930–50.

coral  $\delta^{18}\text{O}$  record before and after the 1970s shift, we select two 20-yr periods (1930–50 and 1975–95). Similar results are obtained when other 20-yr windows centered in the 1930s to the 1960s and after the mid-1970s are considered. The large-scale SST and SLP patterns are constructed by composite maps relative to the interannual component of the coral time series. These maps are defined by averages of SST and SLP fields when the coral  $\delta^{18}\text{O}$  anomaly was greater (smaller) than  $+0.75(-0.75)$  standard deviation. Prior to the composite analysis, both SST and SLP fields are detrended and filtered in the 3–7-year band. We find that the patterns are largely symmetric and show difference maps between the composites for positive and negative coral  $\delta^{18}\text{O}$  anomalies (Figs. 3 and 4). The level of significance of composites is established by means of Student's  $t$  test (von Storch and Zwiers 1999).

The composite maps of SST and SLP show that the interannual variability in the Red Sea coral  $\delta^{18}\text{O}$  is controlled by distinct large-scale atmospheric circulation and SST patterns in the two considered 20-yr windows.

Consistent with the positive correlation between coral  $\delta^{18}\text{O}$  and the Niño-3 index for the period 1975–95 (Fig. 2), a typical El Niño–SST pattern is observed in the tropical Pacific (Fig. 3a). Relatively high positive SST anomalies appear also in the western part of the subtropical North Pacific and along the east coast of North America and the west coast of Europe. The SST anomalies along the west coast of Europe, in the eastern Mediterranean, the eastern tropical Pacific and in some small regions in the subtropical North Pacific are significant at the 95% level.

The corresponding SLP pattern (Fig. 3b) is dynamically consistent with the SST pattern shown in Fig. 3a. Over the Pacific–North American sector, a wave train with a low pressure center over the west coast of the North American continent, a high pressure center over the Labrador Sea, and a low pressure center off the coast of Florida is observed (Fig. 3b). The SLP anomalies are significant at the 95% level in the first two centers. The pattern contains elements of the PNA pattern (Wallace and Gutzler 1981) in its positive phase which is enhanced during El Niño years. Furthermore, the anomalous high pressure center (significant at 95% level) over the northwestern Pacific Ocean is related to positive SST anomalies in the western subtropical North Pacific (Fig. 3a). Outside the PNA sector, a meridional pressure dipole with low pressure anomalies over the polar region

and positive anomalies over the midlatitudes is related to high values in coral  $\delta^{18}\text{O}$  over this period (Fig. 3b).

The composite SST map for the period 1930–50 (Fig. 4a) shows a La Niña SST-like pattern in the Pacific Ocean. In the North Atlantic, the SST anomaly pattern contains elements of the SST pattern that accompanies the positive phase of the North Atlantic Oscillation/Arctic Oscillation (NAO/AO; Hurrell 1995; Thompson and Wallace 1998). The SST anomalies greater than about 0.8 K are significant at 95% level. The corresponding SLP pattern (Fig. 4b) is very similar to that of a positive phase of the AO (Thompson and Wallace 1998). The SST and SLP anomalies in the main centers of the SLP patterns are significant at a 95% level.

### c. Shift in ENSO teleconnections

In order to examine the 1970s shift in ENSO teleconnections as detected both in the coral and northern Red Sea SST data (Fig. 2), we construct regression maps of SLP relative to the interannual component of the Niño-3 index. These regression patterns represent the combined effect of both El Niño and La Niña events and are referred as ENSO-related patterns. In order to be parallel with the analysis relative to the coral record, we use the mean values for January/February of the Niño-3 index and SLP data for three 20-yr periods: 1930–50, 1950–70, and 1975–95. In order to use wind data from the reanalysis period starting in 1948 (Kalnay et al. 1996), we have considered an additional period (1950–70) before the 1970s shift in our regression analysis.

The atmospheric circulation pattern obtained from the regression maps of SLP and the Niño-3 index shows a wave-like structure in the Pacific–North American sector with low pressure over the North Atlantic and Europe (Fig. 5). For the periods 1930–50 and 1950–70, low pressure anomalies extended over central Europe and the Mediterranean realm while high pressure anomalies dominate northern and northeastern Europe. For these periods, positive SST anomalies in the northern Red Sea are detected. These SST anomalies are related to the anomalous low pressure over southern Europe and the Mediterranean basin (Figs. 5a and 5b). The signal is stronger during the 1930–50 relative to the 1950–70 period, which is consistent with the decreasing correlation between Niño-3 and local SST (Fig. 2). The regression map of Niño-3 and SLP for the period 1975–95 (Fig. 5c) shows a coherent large-scale circulation pattern, which resembles the ENSO patterns for the pe-

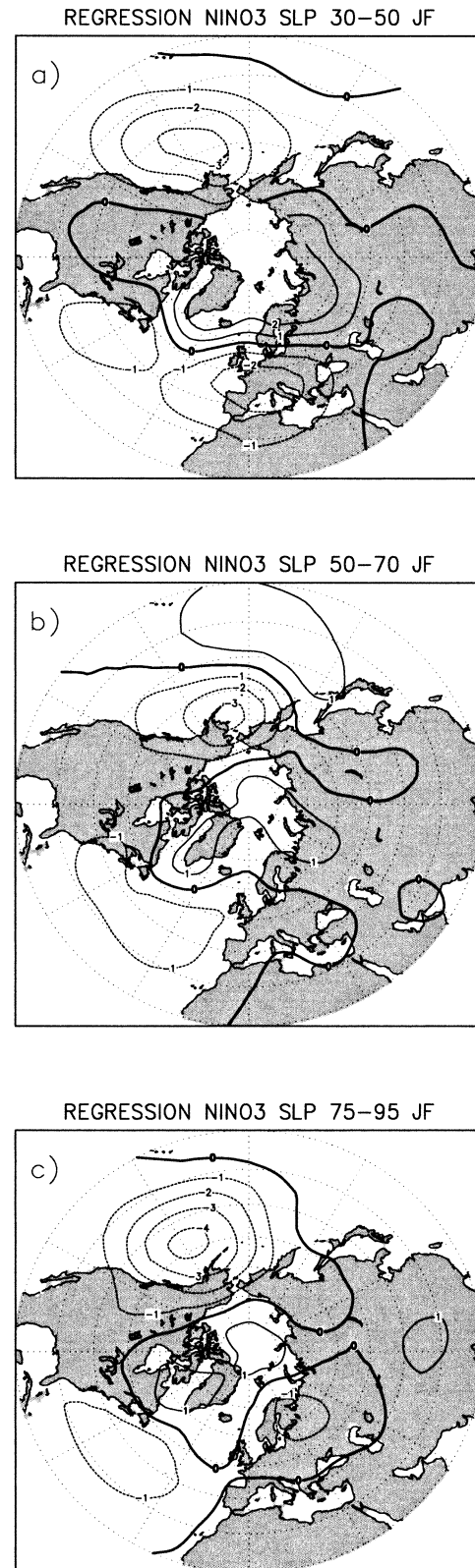


FIG. 5. Regression maps of Northern Hemisphere sea level pressure (Trenberth and Paolino 1980) and the Niño-3 time series for the periods (a) 1930–50, (b) 1950–70, and (c) 1975–95. The data were detrended and filtered in the 3–7-yr frequency interval prior to regression analysis. Units are hPa.

riods prior to the 1970s shift (Figs. 5a and 5b). The low pressure system over the North Atlantic is more westward, and over Europe it is displaced northward relative to the corresponding center in the periods prior to the 1970s shift. Due to these displacements the ENSO teleconnection produces negative SST anomalies over the northern Red Sea. Further analyses show that our results are stable when data from December–February instead of January–February are used to define winter means.

The ENSO-related patterns over Europe during the first two periods emphasize positive SLP anomalies over northern and northeastern Europe and negative SLP anomalies over central and southern Europe consistent with the SLP patterns from El Niño minus La Niña composite maps over the instrumental period (Fraedrich 1994; Pozo-Vázquez et al. 2001). In contrast, the SLP pattern over Europe associated with ENSO events for the period 1975–95 (Fig. 5c) shows negative pressure over large parts of Europe, including northern and northeastern Europe. It also resembles the El Niño SLP pattern for the period 1981–98 as simulated with a high-resolution atmospheric general circulation model (Merkel and Latif 2002).

In order to better assess the SLP anomaly pattern over Europe associated with ENSO, we construct the regression maps of regional SST and 850-mb wind with the Niño-3 time series. Over the period 1950–70 (Fig. 6a), regional wind and SST patterns show an anomalous advection of warm air from the southwest over the northern Red Sea inducing positive SST anomalies. These positive SST anomalies are associated with negative anomalies in the coral  $\delta^{18}\text{O}$  explaining the negative correlation between coral  $\delta^{18}\text{O}$  and the Niño-3 time series over this period (Fig. 2). During the 1975–95 period (Fig. 6b), the anomalous regional circulation related to ENSO is in such a way that cold air is advected from the north over the northern Red Sea (Fig. 6b) explaining the positive correlation between coral  $\delta^{18}\text{O}$  and the Niño-3 index. These regional patterns are compatible with the corresponding large-scale circulation patterns presented in Fig. 5 and are consistent with observed changes in ENSO teleconnections over the Middle East during the mid-1970s (Price et al. 1998).

#### d. Teleconnections with coral records from the tropical Pacific

In order to bring the 1970s shift into a long-term context, we evaluate the shifts in ENSO teleconnections over Europe and the Middle East during the 1750–1995 period based on the northern Red Sea coral  $\delta^{18}\text{O}$  record (Felis et al. 2000) and two coral records from the Pacific Ocean (Urban et al. 2000; Linsley et al., 2000). The variability of the coral  $\delta^{18}\text{O}$  record from Maiana is strongly related to local precipitation, which in turn is linked to SST variability in the Niño-3 region (Urban et al. 2000). The correlation between this time series and global SST at interannual timescales (Fig. 7a) em-

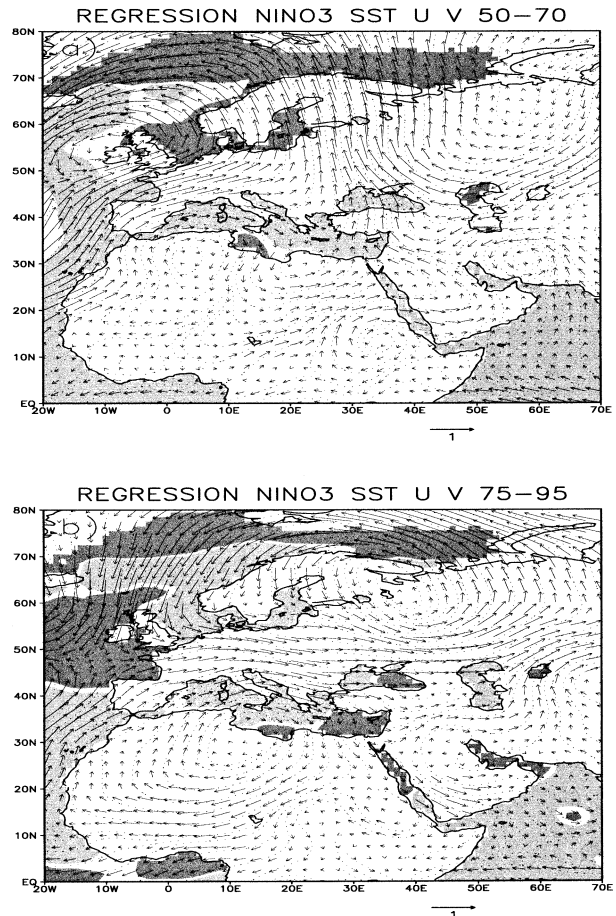


FIG. 6. Regression maps of 850-hPa wind (Kalnay et al. 1996; vectors) and sea surface temperature (Rayner et al. 1996; dark shaded is negative; light shaded is positive) with the Niño-3 index for the period (a) 1950–70 and (b) 1975–95. The data were detrended and filtered in the 3–7-yr frequency band prior to the analysis. Units are  $\text{m s}^{-1}$ .

phasizes a clear ENSO pattern in the tropical Pacific with some connections to the Atlantic and Indian Oceans. This coral  $\delta^{18}\text{O}$  time series has a correlation with SSTs in the Niño-3 region of about  $-0.7$  over the period 1856–1991 (significant at the 95% level). The other time series analyzed here is the Sr/Ca record from Rarotonga (subtropical South Pacific), which reflects changes in local SST (Linsley et al. 2000). It shows an ENSO pattern at interannual timescales with a correlation of about  $0.4$  with SSTs in the Niño-3 region (Fig. 7b).

In analogy to Fig. 2, we evaluate the running correlation coefficients between the tropical Pacific coral time series and the northern Red Sea coral record (Fig. 7c). The running correlation curves for the coral time series show a similar nonstationary behavior compared to the Niño-3–northern Red Sea SST relation during the instrumental period (Fig. 2). Interestingly, shifts are observed in the 1970s, 1920s, 1900s, 1860s, and in the

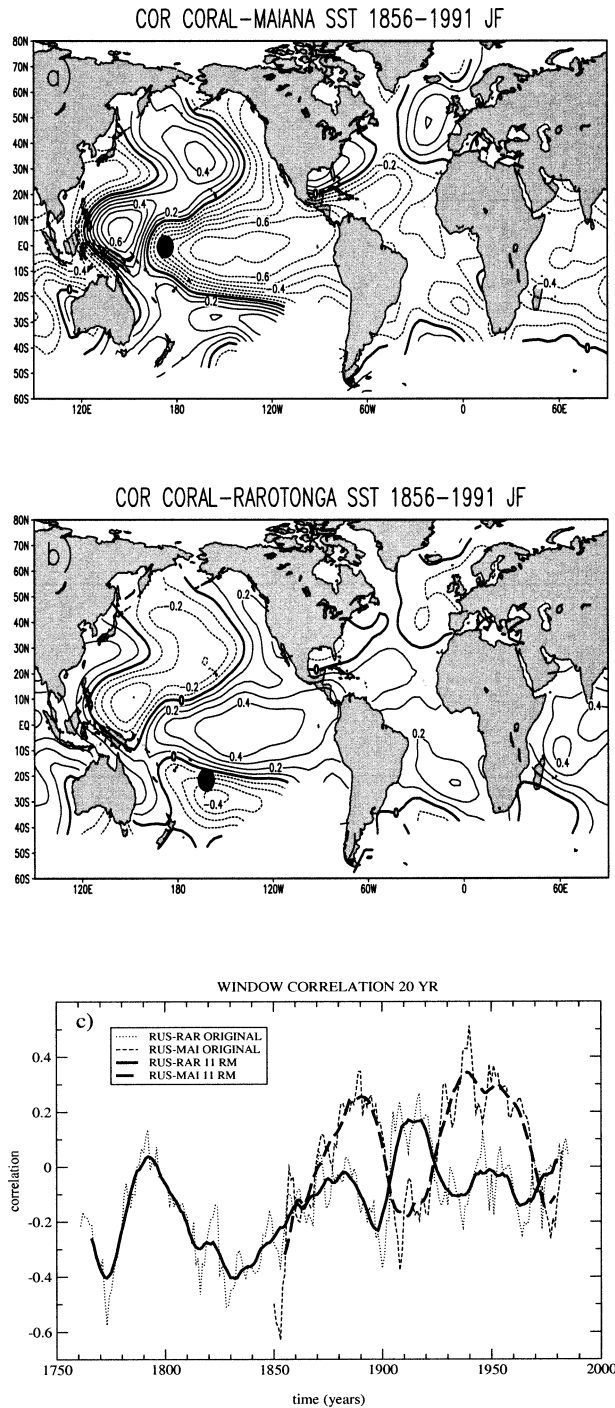


FIG. 7. (a) Correlation map of the coral  $\delta^{18}\text{O}$  time series from Maiana (Linsley et al. 2000) and global sea surface temperature (Kaplan et al. 1998) during JF. (b) Correlation map of the coral Sr/Ca time series from Rarotonga (Urban et al. 2000) and global sea surface temperature during winter. The period of correlation is 1856–1991. Coral locations in (a) and (b) are indicated by black circles. (c) The 20-yr running correlation coefficients between the Ras Umm Sidd coral  $\delta^{18}\text{O}$  record and the coral records from Maiana (dashed line) and Rarotonga (dotted line) during the winter season. To emphasize the shifts the two curves were smoothed with an 11-yr running mean filter (thick lines). The data were detrended and filtered in the 3–7-yr frequency interval prior to the correlation.

1790s. These shifts bring the 1970s climate change into a long-term context.

#### 4. Discussion and conclusions

The coral record from the northern Red Sea shows enhanced and reduced phases of low-frequency variability in a similar way as ice core data (Appenzeller et al. 1998; Moore et al. 2001). In order to analyze the nonstationary response, we investigate the atmospheric circulation and SST anomalies associated with interannual variability recorded by this coral. The window correlation between Red Sea coral  $\delta^{18}\text{O}$  and the Niño-3 index for the period 1856–1995 shows several shifts. We investigate the physical processes that explain the shift from negative to positive correlations between the Niño-3 index and Red Sea coral  $\delta^{18}\text{O}$  time series that occurred in the 1970s.

By analyzing the circulation patterns associated with interannual variability in the Red Sea coral record, we show that over the Atlantic–European region, both before and after the 1970s, the large-scale atmospheric pattern associated with positive anomalies in the coral  $\delta^{18}\text{O}$  record consists of a dipolar structure with negative pressure anomalies over the polar region and high pressure anomalies over the midlatitudes. On the regional scale, this circulation produces a cold air advection from the north toward the northern Red Sea recorded as positive anomalies of  $\delta^{18}\text{O}$  in the Red Sea coral record. The weakly stratified water column of the northern Red Sea provides a favorable condition for monitoring local atmospheric variability (Felis et al. 1998; Eshel et al. 2000), which is in turn related to regional and global circulation regimes (Rimbu et al. 2001).

From the mid-1930s to late 1960s, that is, before the 1970s shift, a PNA-like pattern in its negative phase is associated with positive  $\delta^{18}\text{O}$  anomalies in the Red Sea coral record, providing for a Northern Hemisphere circulation pattern similar to that of the Arctic Oscillation. The negative phase of the PNA is compatible with cold (La Niña) conditions in the tropical Pacific which are associated with positive coral  $\delta^{18}\text{O}$  anomalies during this period (Fig. 4). During this period, we see a strong Pan-Pacific–Atlantic circulation regime. After the 1970s shift, positive anomalies in the Red Sea coral  $\delta^{18}\text{O}$  are related to El Niño conditions. A PNA-like pattern in its positive phase is associated to anomalously cold-air advection over the eastern Mediterranean and Red Sea (Fig. 3). This instability in the patterns associated with interannual variability in the coral record during the two periods reflects changes in the teleconnections between the Pacific and European climate that occurred in the 1970s.

The 1970s shift observed in the correlation between the Niño-3 index and local SSTs and the coral  $\delta^{18}\text{O}$  record (Fig. 2) is a result of changes in the ENSO teleconnections over Europe and the Middle East. These teleconnections may be affected both by changes in the

properties of ENSO itself as well as by changes in the climatic conditions outside the tropical Pacific. Recent studies (An and Wang 2000; Wang and An 2001) show that the dominant period of El Niño increased from 2–3 years during 1960s, and 1970s to 4–5 years during 1980s and 1990s. During this time, the amplitude of El Niño also increased consistent to a stronger Aleutian Low in this period. Similar changes as in the mid-1970s (Stephens et al. 2001) are detected in instrumental data also in the 1940s and 1920s (Zhang et al. 1997). These shifts, which characterize the entire Pacific variability (Zhang et al. 1997), are possibly related to the phase locking of different periodicities in the climate system (Minobe 1999). Proxy data show also a nonstationary behavior of Pacific climate. Gedalof and Smith (2001) find shifts in the North Pacific climate during the past 400 years analyzing tree-ring chronologies from coastal western North America. A similar behavior of North Pacific climate variability has been identified in an annually resolved ice core record from the west coast of North America (Moore et al. 2001). The ENSO teleconnections over Europe are likely to be transmitted via the North Atlantic in association with changes in the mean state of the North Atlantic storm tracks (Merkel and Latif 2002; Pozo-Vázquez et al. 2001). A recent study (Walter and Graf 2002) shows that oceanic and atmospheric conditions in the North Atlantic changed in the late 1960s and early 1970s, which may also contribute to the changes in ENSO teleconnections over Europe.

The ENSO impact over Europe was also investigated in modeling studies (Fraedrich 1994; Dong et al. 2000; Merkel and Latif 2002). The model responses to a particular ENSO event can vary due to different characteristics of particular ENSO events (Dong et al. 2000), as well as due to the model characteristics (Merkel and Latif 2002). Recently, Merkel and Latif (2002) performed an ensemble integration of a high-resolution atmospheric general circulation model forced with global SST patterns obtained by regressing observed winter (December–February) SST anomalies onto the winter Niño-3 index for the period 1981–98. The resulting circulation pattern over Europe is qualitatively similar to our ENSO–SLP regression pattern after the 1970s shift. Longer simulations with such high-resolution models seem to be necessary to detect decadal variations in ENSO teleconnections over Europe as observed in the 1970s. Raible et al. (2001) analyzed a 600-yr experiment with an ocean–atmosphere coupled model and detected two different regimes of the North Atlantic atmospheric circulation connected to the strength of decadal variability in the NAO. One regime is characterized by La Niña conditions and a strong PNA pattern linking the tropical Pacific with the North Atlantic (their global mode). This global mode can be associated with the period of 1930s to 1950s according to our analysis. The other regime (a regional North Atlantic mode in their model experiments) is characterized by a strong decadal

NAO variability and a weaker influence of tropical Pacific processes on the North Atlantic realm, which can be associated to the observed conditions after the 1970s shift. Analogous to our finding, the correlation between NAO and the temperature in the eastern tropical Pacific has different signs in the two regimes in Raible et al.'s (2001) coupled ocean–atmospheric model simulation. The signal communication between the Pacific and Atlantic sectors is possibly linked to modulations of ENSO teleconnections over the European–Middle Eastern realm as detected in our Red Sea coral.

Our results imply that the reconstruction of Northern Hemisphere atmospheric circulation modes from instrumental and proxy climate data, commonly known as an upscaling technique (von Storch and Zwiers 1999), is limited by the nonstationary behavior of teleconnections. The drop or shift in correlations makes the interpretation of such records difficult. Instead, high-resolution proxy records like coral time series from the northern Red Sea (Felis et al. 2000) and from the tropical Pacific (Linsley et al. 2000; Urban et al. 2000) can bring climate shifts, like that from 1970s, into a long-term context. The observed nonstationarity in the extratropical response to ENSO seems to be a general phenomenon. Ice cores (e.g., Moore et al. 2001), as well as tree rings (Gedalof and Smith 2001), show intermittent coherent patterns on interdecadal timescales. Furthermore, it is conceivable that the degree of predictability of ENSO teleconnections is strongly limited by these modulations. The logical next step would be to extend our analysis to other annually resolved archives like ice cores, tree rings, varved sediments, and speleothems in order to understand long-term climate shifts and related teleconnections.

*Acknowledgments.* We would like to thank G. Wefer and K. Herterich for their support. Discussions with K. Grosfeld and M. Dima have been valuable. The authors would like to acknowledge A. Manschke for computing assistance. This work was supported by the German government through DEKLIM.

#### REFERENCES

- An, S.-I., and B. Wang, 2000: Interdecadal changes in the structure of ENSO mode and its impact on the ENSO frequency. *J. Climate*, **13**, 2044–2055.
- Appenzeller, C., T. F. Stocker, and M. Anklin, 1998: North Atlantic Oscillation dynamics recorded in Greenland ice cores. *Science*, **282**, 446–449.
- Charles, C. D., D. E. Hunter, and R. G. Fairbanks, 1997: Interaction between the ENSO and the Asian monsoon in a coral record of tropical climate. *Science*, **277**, 925–928.
- Cole, J. E., R. G. Fairbanks, and G. T. Shen, 1993: Recent variability in the Southern Oscillation: Isotopic results from a Tarawa Atoll coral. *Science*, **260**, 1790–1793.
- Dong, B. W., R. T. Sutton, S. P. Jewson, A. O'Neill, and J. M. Slingo, 2000: Predictable winter climate in the North Atlantic sector during the 1997–1999 ENSO cycle. *Geophys. Res. Lett.*, **27**, 985–988.
- Eshel, G., D. P. Schrag, and B. F. Farrell, 2000: Troposphere–planetary

- boundary layer interactions and the evolution of ocean surface density: Lessons from Red Sea corals. *J. Climate*, **13**, 339–351.
- Evans, M. N., M. A. Cane, D. P. Schrag, A. Kaplan, B. K. Linsley, R. Villalba, and G. M. Wellington, 2001: Support for tropically-driven Pacific decadal variability based on paleoproxy evidence. *Geophys. Res. Lett.*, **28**, 3689–3692.
- Felis, T., J. Pätzold, Y. Loya, and G. Wefer, 1998: Vertical water mass mixing and plankton blooms recorded in skeletal stable carbon isotopes of a Red Sea coral. *J. Geophys. Res.*, **103**, 30 731–30 739.
- , —, —, M. Fine, A. H. Nawar, and G. Wefer, 2000: A coral oxygen isotope record from the northern Red Sea documenting NAO, ENSO, and North Pacific teleconnections on Middle East climate variability since the year 1750. *Paleoceanography*, **15**, 679–694.
- Fraedrich, K., 1994: An ENSO impact on Europe? *Tellus*, **46A**, 541–552.
- , and K. Müller, 1992: Climate anomalies in Europe associates with ENSO extremes. *Int. J. Climatol.*, **12**, 25–31.
- Gedalof, Z., and D. J. Smith, 2001: Interdecadal climate variability and regime-scale shifts in Pacific North America. *Geophys. Res. Lett.*, **28**, 1515–1518.
- Hamilton, K., 1988: A detailed examination of the extratropical response to tropical El Niño/Southern Oscillation events. *J. Climatol.*, **8**, 67–86.
- Huang, J., K. Higuchi, and A. Shabbar, 1998: The relationship between the North Atlantic Oscillation and El Niño–Southern Oscillation. *Geophys. Res. Lett.*, **25**, 2707–2710.
- Hurrell, J. W., 1995: Decadal trends in the North Atlantic Oscillation: Regional temperatures and precipitation. *Science*, **269**, 676–679.
- Kalnay, E. M., and Coauthors, 1996: The NCEP/NCAR 40-Year Reanalysis Project. *Bull. Amer. Meteor. Soc.*, **77**, 437–471.
- Kaplan, A., M. Cane, Y. Kushnir, A. Clement, M. Blumenthal, and B. Rajagopalan, 1998: Analyses of global sea surface temperature 1856–1991. *J. Geophys. Res.*, **103**, 18 567–18 589.
- Linsley, B. K., G. M. Wellington, and D. P. Schrag, 2000: Decadal sea surface temperature variability in the subtropical South Pacific from 1726 to 1997 A.D. *Science*, **290**, 1145–1148.
- Mariotti, A., N. Zeng, and K. M. Lau, 2002: Euro-Mediterranean rainfall and ENSO—A seasonally varying relationship. *Geophys. Res. Lett.*, **29**, 1621, doi:10.1029/2001GL014248.
- Merkel, U., and M. Latif, 2002: A high resolution AGCM study of the El Niño impact on the North Atlantic/European sector. *Geophys. Res. Lett.*, **29**, 1291, doi:10.1020/2001GL013726.
- Minobe, S., 1999: Resonance in bidecadal and pentadecadal climate oscillations over the North Pacific: Role in climatic regime shifts. *Geophys. Res. Lett.*, **26**, 855–858.
- Moore, G. W. K., G. Holdsworth, and K. Alverson, 2001: Extratropical response to ENSO as expressed in an ice core from the Saint Elias mountain range. *Geophys. Res. Lett.*, **28**, 3457–3460.
- Pozo-Vázquez, D., M. J. Esteban-Parra, F. S. Rodrigo, and Y. Castro-Diez, 2001: The association between ENSO and winter atmospheric circulation and temperature in the North Atlantic region. *J. Climate*, **14**, 3408–3420.
- Price, C., L. Stone, A. Huppert, B. Rajagopalan, and P. Alpert, 1998: A possible link between El Niño and precipitation in Israel. *Geophys. Res. Lett.*, **25**, 3963–3966.
- Raible, C., U. Luksch, K. Fraedrich, and R. Voss, 2001: North Atlantic decadal regimes in a coupled GCM simulation. *Climate Dyn.*, **18**, 321–330.
- Rayner, N. A., E. B. Horton, D. E. Parker, C. K. Folland, and R. B. Hackett, 1996: Version 2.2 of the global sea-ice and sea surface temperature data set, 1903–1994. Climate Research Tech. Note 74, Hadley Centre, Met Office, Bracknell, United Kingdom, 43 pp.
- Rimbu, N., G. Lohmann, T. Felis, and J. Pätzold, 2001: Arctic Oscillation signature in a Red Sea coral. *Geophys. Res. Lett.*, **28**, 2959–2962.
- , —, —, and —, 2003: Detection of climate modes in a seasonal resolution coral record covering the last 250 years. *The KIHZ Project: Toward a Synthesis of Holocene Proxy Data and Climate Models*, H. Fischer et al., Eds., Springer-Verlag, in press.
- Rodo, X., E. Baert, and F. A. Comin, 1997: Variations in seasonal rainfall in Southern Europe during the present century: Relationships with the North Atlantic Oscillation and the El Niño–Southern Oscillation. *Climate Dyn.*, **13**, 275–284.
- Stephens, C., S. Levitus, J. Antonov, and T. P. Boyer, 2001: On the Pacific Ocean regime shift. *Geophys. Res. Lett.*, **28**, 3721–3724.
- Thompson, D. W. J., and J. W. Wallace, 1998: The Arctic Oscillation signature in the wintertime geopotential height and temperature fields. *Geophys. Res. Lett.*, **25**, 1297–1300.
- Torrence, C., and G. P. Compo, 1998: A practical guide to wavelet analysis. *Bull. Amer. Meteor. Soc.*, **79**, 61–78.
- Trenberth, K. E., and D. A. Paolino, 1980: The Northern Hemisphere sea-level pressure data set: Trends, errors and discontinuities. *Mon. Wea. Rev.*, **108**, 855–872.
- Urban, F. E., J. E. Cole, and J. T. Overpeck, 2000: Influence of mean climate change on climate variability from a 155-year tropical Pacific coral record. *Nature*, **407**, 989–993.
- van Loon, H., and R. A. Madden, 1981: The Southern Oscillation. Part 1: Global associations with pressure and temperature in Northern Hemisphere winter. *Mon. Wea. Rev.*, **109**, 1150–1162.
- von Storch, H., and F. W. Zwiers, 1999: *Statistical Analysis in Climate Research*. Cambridge University Press, 484 pp.
- Wallace, J. M., and D. S. Gutzler, 1981: Teleconnections in the geopotential height field during the Northern Hemisphere winter. *Mon. Wea. Rev.*, **109**, 784–812.
- Walter, K., and H. F. Graf, 2002: On the changing nature of the regional connection between the North Atlantic Oscillation and sea surface temperature. *J. Geophys. Res.*, **107**, 4338, doi:10.1029/2001JD000850.
- Wang, B., and S.-I. An, 2001: Why the properties of El Niño changed during the late 1970s. *Geophys. Res. Lett.*, **28**, 3709–3712.
- Zhang, Y., J. M. Wallace, and D. S. Battisti, 1997: ENSO-like interdecadal variability: 1900–93. *J. Climate*, **10**, 1004–1020.